AAS 12-104

OPTIMAL RECONFIGURATIONS OF COULOMB FORMATIONS ALONG INVARIANT MANIFOLDS

D.R. Jones*

Coulomb formations refer to swarms of closely-flying spacecraft, in which the net electric charge of each vehicle is controlled. Active charge control is central to this concept and enables a propulsion system with highly desirable characteristics, albeit with limited controllability. Numerous Coulomb equilibria have been derived (for various force models), but to maintain and maneuver these configurations, some inertial thrust is required to supplement the nearly propellant-less charge control. In this work, invariant manifold theory is applied to dynamically unstable Coulomb configurations, as part of a generalized procedure to formulate and parameterize optimal transfers from one Coulomb configuration to another. The emphasis is on minimizing the inertial thrust necessary to complete such reconfigurations, in part, by exploiting uncontrolled motion along the manifolds. The possible permutations and variations for modeling the optimal transfers, that are within the scope of the general methodology, are discussed. Numerical results are then provided, as demonstrative examples of the optimization procedure, using a two-craft Coulomb formation model with linearized two-body gravity and simple control parameterizations. Particle Swarm Optimization, a novel stochastic method, is used to solve the optimal transfer problems and its adeptness at doing so, as well as its additional utility in Coulomb formation research, is addressed.

INTRODUCTION

Close-proximity formations of cooperative spacecraft (s/c) are being considered for a variety of applications, and have many advantages over a single large craft, including: overall mass reduction, the ability to be deployed and assembled on multiple launches, and a unique ability to perform scientific tasks such as interferometry. The NASA Terrestrial Planet Finder Mission (TPF) is one example in which this concept is being proposed.[1] Existing electric propulsion (EP) systems have been considered to control relative formation motions; however, EP suffers from limited throttle-ability and introduces the problem of thruster-plume impingement. The latter problem involves EP thruster ejecta damaging neighboring craft and is especially detrimental at small separation distances (order of meters).[2] Coulomb thrusting was recently introduced by King et. al.[2−3] as an alternative to EP, where the electric potential (or net charge) of each s/c is actively controlled, to provide inter-craft forces. It was demonstrated that such a propulsion system could provide the static equilibrium forces (on the order of μN-mN), necessary to sustain various 3-5 craft 'virtual structures', and with less power and fuel than competing EP systems.[2] In fact, the Coulomb configurations simulated in this work had power requirements on the order of 0.1 W and fuel usage on the order of 10 grams, for 10-year operations. Furthermore, this nearly-propellant-less system (*ISP* as high as 10^{13} sec) averts thruster-plume impingement, and has extremely fast throttling (max charge transition on the order

*Graduate Student, Department of Aerospace Engineering and Engineering Mechanics, The University of Texas at Austin, 1 University Station C0600, Austin, Texas 78712, Student Member AAS/AIAA

of msec).[2] Also, this concept is made possible using existing technology, since active control of s/c charge was successfully executed during the SCATHA[5] and ATS[6] missions, and currently on the CLUSTER[7] mission. Other potential applications for active charge control have been suggested including: advanced docking/rendezvous, autonomous inspection, contact-less removal of hazardous material, and the deployment/retrieval of instruments.[4]

Unfortunately, this type of propulsion system does have a couple of drawbacks. First, the system's ability to generate useful force magnitudes may be infeasible in some environmental regimes (due to the local plasma screening the electric potential's 'sphere-of-influence' down to impractical distances). This is primarily troublesome at LEO, but much less so at GEO and interplanetary distances. The second drawback is that Coulomb thrusting alone provides limited controllability, and cannot alter the overall formation angular momentum.[8] This has led to the adoption of hybrid propulsion systems, where charge control is supplemented with inertial thrust (EP or chemical) to enable full controllability.[9−10] Many constant-charge equilibrium configurations have been derived (analytically for formations with less than 5 s/c, and numerically otherwise), and thus far, all are dynamically unstable.[2−4] Other known Coulomb equilibria include: 3-s/c formations in the absence of gravitational forces,[11] and 2-s/c formations using fully non-linear equations in the restricted 2-body and 3-body (CRTBP) problems.[10] Moreover, these highly nonlinear and coupled dynamical systems permit the potential existence of numerous, yet undiscovered, equilibria and periodicity conditions (constant and/or variable charge).

This research will discuss how invariant manifolds associated with nominal Coulomb formations (static or periodic) may be used in the derivation of station-keeping and maneuvering methods. A novel and generalized procedure for targeting optimal transfers from one Coulomb configuration to another is outlined in detail. In this methodology, a nonlinear program is formulated and the system's uncontrolled flow, along manifolds, is exploited to yield a partial transfer. This then is differentially corrected using parameterized controls to form the continuous trajectory. Generally some measure of fuel or power consumption (but not time) is minimized, since motion along manifolds implies long duration transfers. Furthermore, a new and unique stochastic method, known as Particle Swarm Optimization (PSO), is proposed for solving the optimal reconfigurations, and the advantages of doing so are discussed.[12−13]

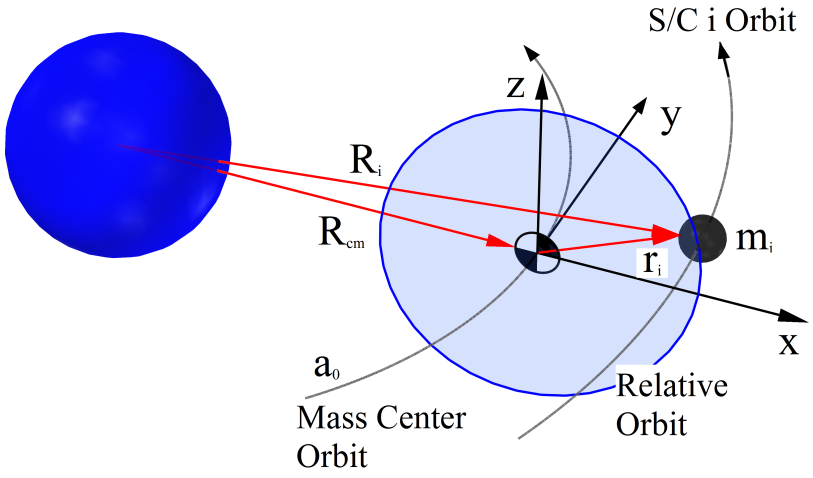

Figure 1. Rotating Hill Coordinate Frame with Relative Position Vector $\mathbf{r}_i$

For Coulomb formations near GEO, a common assumption is to describe s/c motions relative to a nominal center-of-mass (CM) orbit (assumed circular with semi-major-axis a_0 near GEO), using the linearized Clohessy-Wiltshire-Hill (CW) equations of motion.[14] The rotating Hill frame, with origin at CM and axes labeled: x for radial, y for transverse, and z for normal, is depicted in Figure 1. This model admits three equilibrium configurations, such that both craft appear statically fixed with respect to the Hill frame. Inampudi applied a pseudo-spectral discretization method for targeting optimal transfers between these equilibrium configurations, for minimum: time, fuel, and total power usage.[10] This research also pursues optimal transfers (reconfigurations) between the same equilibria; however, the problem setup differs substantially, with added emphasis on generality. The current work also contrasts with that of,[10] by its utilization of invariant manifold theory and employment of a stochastic rather than a deterministic optimization method.

In terms of Coulomb formation stabilization, thus far only continuous feedback controllers have been considered. Such controllers have been derived and tested (in the presence of gravity gradient torque and other disturbances) by Natarajan and Schaub for the 2-s/c Hill frame equilibria,[9,15] and by Inampudi for CRTBP equilibrium configurations about Earth-Moon libration points.[10] Continuous thrusting, however, may not be feasible for all missions. Discrete formation-keeping would be necessary in these cases, and invariant manifold theory enables a class of such methods, which might also yield less overall impulsive cost (ΔV) than continuous approaches. An example method, is the Floquet controller, described in detail by Marchand, in which impulsive maneuvers are applied at discrete intervals in order to eliminate perturbations along unstable manifold modes (allowing the stable modes to return the formation to nominal).[16] In contrast to previously developed methods, this approach cannot ensure asymptotic stability, and depending on the frequency of the maneuvers large tracking errors could result. Discrete stabilization methodologies, as substitutes or supplements to feedback controllers, are not considered in this work; however, the application of invariant manifold theory to Coulomb formations would be useful in their derivation.

COULOMB FORMATION BACKGROUND AND MODELING

Conductive s/c surfaces naturally exchange ions and electrons with the surrounding plasma, and as a result assume a non-zero overall charge q. This net charge generates an electric potential ϕ (measured in Volts and proportional to q), that reaches equilibrium when the net currents in/out are equal to zero (as high as kV magnitude ϕ have developed on operational s/c).[2] In a vacuum, $\phi(r)$ of a charged sphere will decay in proportion to k_c/r, where k_c is the Coulomb constant and r is the distance from the surface center. But in a plasma, the extent of this ideal $\phi(r)$ is effectively limited (or shielded) due to interactions with free particles and photons. The Debeye length λ_d is often used to parameterize this shielding, such that a charged particle outside a sphere of radius λ_d will not be effected by a $\phi(r)$ centered at $r = 0$. The Debeye length is a measure of the time-dependent local plasma temperature and density, and experimental values for it have been acquired in various regimes (e.g. LEO: $0.02 - 0.4$ m, GEO: $140 - 1500$ m, Interplanetary: $7.4 - 24$ m).

Numerous authors have presented high fidelity computations of ϕ for realistic s/c, using finite element analysis techniques and/or experimental data, and the true ϕ is modeled by the Vlaslov-Poisson partial differential equations.[3,17,18] In particular, Stiles, Seubert, and Schaub showed that the potential is bounded above by the vacuum model and below by the conservative Debeye-Hückel model (a truncated version of the Vlaslov-Poisson equations).[17] For the current research, each s/c is modeled as a sphere with radius R_{sc} with an outer conducting surface of uniform charge density, and it is assumed that $R_{sc} \ll \lambda_d$ (generally valid at GEO). By also assuming that s/c separation

distances r_{ij} are greater than $10R_{sc}$, each s/c ϕ may be modeled in simple proportion to its net charge q as given by Eq. (1).

$$\phi = k_c \frac{q}{R_{sc}} \tag{1}$$

More complex analytic expressions have been derived for scenarios in which these assumptions are invalid, and could always be adopted in such cases.[17] Nevertheless, these assumed conditions are enforced throughout this work, allowing each s/c to be modeled accurately as equivalent point charges, using a simplified version of the Debeye-Hückel model, given by Eq. (2). This provides a simple analytical expression for the potential of a s/c j with overall charge q_j at a distance r, with partial shielding.

$$\phi_j(r) = k_c \frac{q_j}{r}\, e^{-r/\lambda_d} \tag{2}$$

It should be noted that in practice ϕ is the control, since it is readily measured; however, with these assumptions the net charge q may be considered as a control.

Active Charge Control Background

Altering s/c ϕ artificially, simply involves utilizing an electron-gun or similar device to emit electrons/ions into the surrounding plasma, and this process has substantial mission heritage.[5–7] To achieve and maintain an arbitrary ϕ, the ejected particles must depart with sufficient kinetic energy to escape the generated 'potential-well', and do so at a rate greater than the incoming environmental current I_{en} (since this will tend to drive ϕ back towards natural equilibrium). Therefore, the device must have sufficient power P to supply a voltage equal to the desired ϕ, at a current I_{out} at least greater than I_{en}. Therefore combining Ohm's law with Eq. (1) yields Eq. (3), an expression for the device power P and the time required Δt_q to change the net charge by an amount $|\Delta q|$.

$$P = \phi\, I_{out} \qquad \Delta t_q = \frac{|\Delta q|}{I_{out}} = \frac{R_{sc}|\Delta\phi|}{k_c\, I_{out}} \tag{3}$$

General Coulomb Formation Force Model

The force exerted on another s/c i with net charge q_i, due to ϕ_j, is then simply q_i times the gradient of ϕ_j, given by Eq. (2), with respect to the vector $\mathbf{r}_i$. Eqs. (4a)-(4b) are used in this work to model the total acceleration of s/c i, with the $\mathbf{H_i}$ term denoting Coulomb accelerations resulting from all other charged craft. The distance between s/c i and s/c j is denoted $r_{ij} = \|\mathbf{r_i} - \mathbf{r_j}\|$, $\mathbf{G_i}$ accounts for natural acceleration terms (e.g. gravity), and $\mathbf{u_i}$ denotes any controllable inertial acceleration.

$$\mathbf{H_i} = \frac{\mathbf{f_i}}{m_i} = \frac{k_c\, q_i}{m_i} \sum_{j \neq i} \frac{q_j\, e^{-r_{ij}/\lambda_d}}{r_{ij}^3} \left(1 + \frac{r_{ij}}{\lambda_d}\right) \mathbf{r_{ij}} \tag{4a}$$

$$\ddot{\mathbf{r}}_\mathbf{i} = \mathbf{H_i} + \mathbf{G_i} + \mathbf{u_i} \tag{4b}$$

Furthermore, any Coulomb formation of arbitrary number of s/c may be described by a 1st order ODE system, denoted $\dot{\mathbf{X}} = \mathbf{F}(\mathbf{X},\ \mathbf{X_p},\ t)$, where t is the independent variable of integration (assumed time). The state vector $\mathbf{X}$, of dimension N, includes the position and velocity vectors for each s/c $\mathbf{r_i}$ and $\mathbf{v_i}$, and possibly each s/c mass m_i (if variable). The elements of $\mathbf{X_p}$ may be constant or t dependent, and will include the control functions for each s/c: inertial thrust $\mathbf{u_i}(t)$ and Coulomb thrust (defined using $\phi_i(t) \rightarrow q_i(t)$). Small state perturbations $\delta\mathbf{X}$ about some reference solution

$\mathbf{X}^*$, may be considered as defined by Eq. (5), where $\mathbf{X}^*$ may be: an equilibrium configuration, a periodic motion, or simply a nominal trajectory.

$$\delta\dot{\mathbf{X}} = \left(\frac{\partial \mathbf{F}}{\partial \mathbf{X}}\right)\Bigg|_{\mathbf{X}^*} \delta\mathbf{X} = \mathbf{A}\,\delta\mathbf{X} \tag{5}$$

This yields a linearized ODE system for the perturbation vector $\delta\mathbf{X}$, where $\mathbf{A}$ is the Jacobian matrix that can be transformed to Jordan canonical form: $\mathbf{A} = \mathbf{S}[\Lambda]\mathbf{S}^{-1}$. Where, $[\Lambda]$ is a block-diagonal matrix whose entries are the eigenvalues of $\mathbf{A}$, and $\mathbf{S}$ has columns corresponding to the normalized eigenvectors of $\mathbf{A}$. The columns or modes of $\mathbf{S}$, allow the Jacobian matrix to be decomposed into unstable, stable, and center eigenspaces (E^u, E^s, E^c with dimensions N_u, N_s, and N_c, respectively) such that $N = N_u + N_s + N_c$. In this linearized system, perturbations with components along the E^u basis vectors will tend to grow, those in E^s will tend to dissipate, and those in E^c will neither increase or decrease.

Two-Craft Coulomb Formation Model

The following 2-s/c Coulomb formation model, using the linearized CW equations of motion,[14] is used to numerically demonstrate the proposed optimization methodology of this research. The gravitational acceleration of s/c 1, with respect to the formation CM ($\mathbf{G_1}$), is defined by Eq. (6a), and the Eq. (6b) condition is imparted from assuming the Hill frame origin to be at the CM.

$$\mathbf{G_1} = \begin{bmatrix} 2\omega\dot{y}_1 + 3\omega^2 x_1 \\ -2\omega\dot{x}_1 \\ -\omega^2 z_1 \end{bmatrix} \tag{6a}$$

$$0 = m_1\mathbf{r_1} + m_2\mathbf{r_2} \tag{6b}$$

Where, ω is the nominal CM orbit rate (or Hill frame rotational rate with respect to an inertial frame), and $L = r_{12}$ is the separation distance of the two craft. It is clear from Eq. (6b) that $\mathbf{r_1}$ and $\mathbf{r_2}$ are dependent, and in fact may be related via L using some some mass fractions, as follows:

$$L = \frac{r_1}{M_{r1}} = \frac{r_2}{M_{r2}} \qquad L = \|\mathbf{r_1} - \mathbf{r_2}\| \qquad M_{r1} = \frac{m_2}{m_1 + m_2} \qquad M_{r2} = \frac{m_1}{m_1 + m_2}$$

A further assumption (as done in[15,11]) is made that: $L/\lambda_d << 1$, such that the $(1 + r_{12}/\lambda_d)$ term in Eq. (4a) may be ignored. This assumption has been shown to be very accurate at GEO, so long as L is less than 50 or ever 100 meters.[2,10] Therefore, only separation distances L on the order of tens of meters are considered. Eq. (7a) is then the result of this assumption, and the substitution of Eq. (6b) into Eq. (4a) to eliminate the s/c 2 state from $\ddot{\mathbf{r}}_\mathbf{1}$.

$$\ddot{\mathbf{r}}_\mathbf{1} = \mathbf{G_1} + \mathbf{H_1} = \begin{bmatrix} 2\omega\,\dot{y}_1 + 3\omega^2 x_1 + \frac{\kappa_1\, Q\, x_1}{r_1^3\, exp[r_1/M_{r1}\lambda_d]} \\ -2\omega\dot{x}_1 + \frac{\kappa_1\, Q\, y_1}{r_1^3\, exp[r_1/M_{r1}\lambda_d]} \\ -\omega^2\, z_1 + \frac{\kappa_1\, Q\, z_1}{r_1^3\, exp[r_1/M_{r1}\lambda_d]} \end{bmatrix} \qquad \kappa_1 = \frac{k_c\, M_{r1}^2}{m_1} \tag{7a}$$

$$\mathbf{X_1} = \begin{bmatrix} \mathbf{r_1} \\ \mathbf{v_1} \end{bmatrix} = \begin{bmatrix} x_1 & y_1 & z_1 & v_{x1} & v_{y1} & v_{z1} \end{bmatrix}^T \tag{7b}$$

This expression describes the uncontrolled s/c 1 acceleration as a function of its own state-vector $\mathbf{X_1}$ (defined in Eq. (7b)), and a charge product term Q. Where, $Q = q_1 q_2$ and it is assumed that $|q_1| = |q_2|$. Furthermore, Eq. (7a) completely governs the system, since the motion of s/c 2 may be explicitly computed from s/c 1 using Eq. (6b).

Two-Craft Coulomb Formation Equilibrium Configurations and Stability

Eqs. (6b)-(7a) admit three known static equilibrium configurations which are depicted in Figures 2(a)-2(b) and Figure 3, and are denoted: Radial, Orbit-Normal, and Along-Track. A thorough derivation of the conditions for equilibrium, as summarized in Table 1, can be found in.[4] The required Q to achieve equilibrium is denoted Q_{ref}, and is dependent on m_1, m_2, and the initial separation distance L_0. It is important to note that an attractive force is necessary for the Radial configuration, whereas the Orbit-Normal configuration requires a repulsive force.

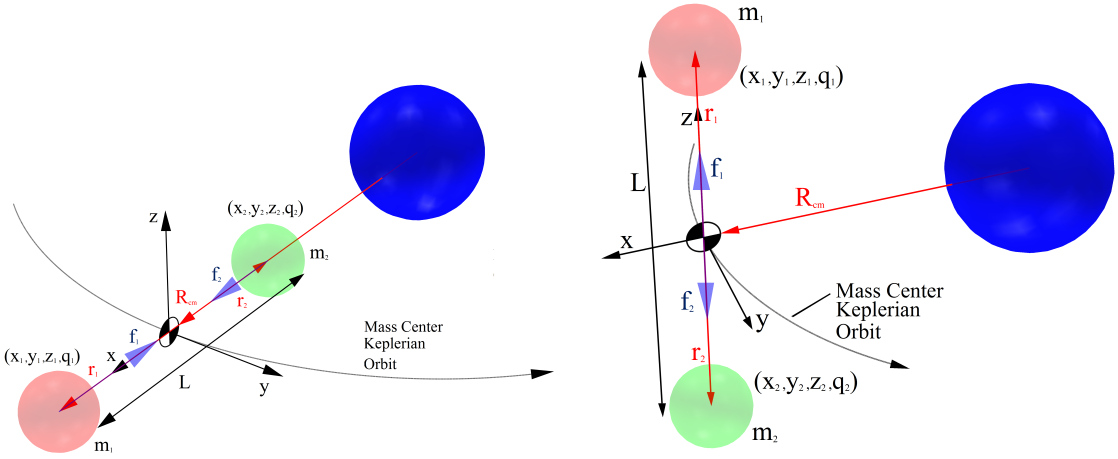

(a) Radial (b) Orbit-Normal

Figure 2. Two-S/C Coulomb Formation Equilibrium Configurations in the Hill Frame

Table 1. Two-Craft Coulomb Formation Equilibrium Condition Summary

Configuration	S/C 1 Pos. Vector, $\mathbf{r_1}$	Charge Product Q_{ref} (C^2)
Radial	$x_1 = y_1 = 0,\ z_1 = M_{r1} L_0$	$\frac{\omega^2\ m_1 m_2\ L_0^3\ e^{(L_0/\lambda_d)}}{k_c\ (m_1+m_2)}$
Orbit-Normal	$y_1 = z_1 = 0,\ x_1 = M_{r1} L_0$	$\frac{-3\omega^2\ m_1 m_2\ L_0^3\ e^{(L_0/\lambda_d)}}{k_c\ (m_1+m_2)}$
Along-Track	$x_1 = z_1 = 0,\ y_1 = M_{r1} L_0$	0

A 1st order ODE system (for either s/c) may then be linearized about each equilibria to arrive at a Jacobian matrix $\mathbf{A}$ (and corresponding Jordan form). The linearized stability properties for each may be entirely determined from the eigenvalues of $\mathbf{A}$; however, an alternative stability analysis was previously performed by Natarajan and Schaub.[9,15] Nevertheless, some important stability properties are summarized as follows:

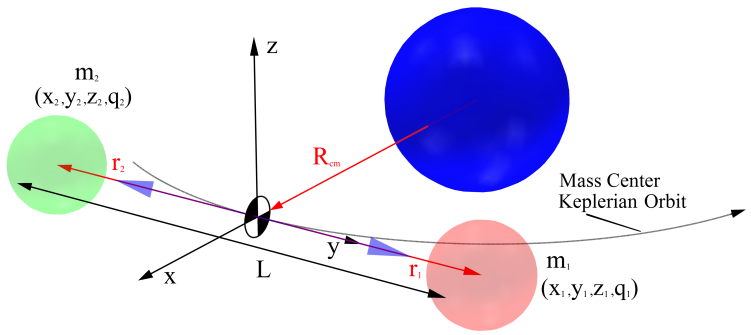

Figure 3. Two-S/C Coulomb Formation Along-Track Equilibrium Configuration in the Hill Frame

1. All three equilibrium configurations are dynamically unstable.

2. The eigenvalues are functions of: m_1, m_2, and ω. However, the stability properties of all configurations remain constant (i.e. there are no bifurcations or changes in N_u, N_s, and N_c).

3. **Radial:** All eigenvalues are distinct. This configuration has one unstable and one stable eigenvalue and both are real ($N_u = N_s = 1$). The stable/unstable eigenvectors are contained in the x-y plane. The dimension of the center eigenspace is $N_c = 4$, with one oscillatory mode in the x-y plane and the other along the z-axis.

4. **Orbit-Normal:** All eigenvalues are distinct. This configuration has an unstable and a stable complex conjugate pair ($N_u = N_s = 2$), resulting in oscillatory modes with components in x, y, and z directions. The center subspace has dimension $N_c = 2$ and is along the z-axis.

5. **Along-Track:** All eigenvalues associated with this configuration have zero real part ($N_c = 6$), but there is a zero modulus repeated eigenvalue with algebraic multiplicity less than geometric multiplicity. The Jordan form then requires a generalized eigenvector, and the mode associated with this vector produces unbounded motion.

INVARIANT MANIFOLD THEORY APPLIED TO COULOMB FORMATIONS

The global stable and unstable manifolds (if they exist) are subspaces containing all trajectories (or flows) governed by the original nonlinear system dynamics (**F**), with the following properties:

1. Unstable manifold (W^u): set of all trajectories which depart $\mathbf{X}^*$ asymptotically as $t \to \infty$.

2. Stable manifold (W^s): set of all trajectories which approach $\mathbf{X}^*$ asymptotically as $t \to -\infty$.

3. The manifolds are invariant, and therefore a state contained within W^u or W^s remains in that subspace for all time (e.g. the flow cannot naturally evolve from W^u to W^s).

4. The manifolds are tangent to their respective eigenspaces, in both $\pm$ directions at each discrete point on $\mathbf{X}^*(\beta_j)$ (there is no β_j for equilibrium points), and the $\pm$ yields two branches of W^u and W^s at each $\mathbf{X}^*(\beta_j)$ point. Also, the manifold subspaces are 1-D higher than their corresponding eigenspaces (i.e. W^u has dimension of $N_u + 1$).

The general procedure for creating the manifolds is to perturb the state by a small amount $\pm\epsilon$, along the normalized eigenvectors which span either E^u or E^s (where applicable, $\mathbf{X}^*$ is discretized into $j = 1 \dots M_{node}$ nodes, and the eigenvectors are determined at each node). For constructing W^u, the perturbed state $\mathbf{X} = \mathbf{X}^*(\beta_j) \pm \epsilon\ E^u(\beta_j)$ is propagated forward in time using $\mathbf{F}$, from $t = 0 \rightarrow t^u_{max}$. Analogously for W^s, the perturbed state $\mathbf{X} = \mathbf{X}^*(\beta_j) \pm \epsilon\ E^s(\beta_j)$ is propagated backward in time from $t = t^s_{max} \rightarrow 0$. Particular unstable and stable manifold states, denoted $\mathbf{X^u}(t^u_i, \beta_j) \in W^u$ and $\mathbf{X^s}(t^s_i, \beta_j) \in W^s$, may be identified using only two time-like parameters: β_j and $t^{u/s}_i$. Where the former denotes discrete points of departure/arrival on $\mathbf{X}^*$ (where applicable), and the latter denotes the time propagation along that manifold branch.

Invariant manifold theory has successfully been used to design low-thrust transfers between regions of space, in multi-body gravity fields, for example in the work of Russell and Lam.[19] Because the manifolds illustrate non-intuitive trajectories, and dynamical motions which are otherwise difficult to visualize, analogous benefits might result from their application to Coulomb formations. The use of manifolds in this paper is restricted to designing trajectories which 'hop' from unstable to stable branches in order to partially achieve formation reconfigurations, hopefully with low cost. However, it should be noted that the theory has utility in other areas. For example, the local manifolds describe how flows depart or approach some nominal configuration, and therefore would be instrumental in designing a discrete controller to eliminate perturbations along unstable manifolds, while intensifying those along stable manifolds.

GENERALIZED METHODOLOGY FOR TARGETING OPTIMAL COULOMB RECONFIGURATIONS ALONG MANIFOLDS

The primary objective in this research, is to develop a method to maneuver from some charged s/c configuration to another, with minimal: power, total ΔV, or fuel use. To do this, uncontrolled flows along manifolds, that complete as much of the transfer as possible, are sought and provide a discontinuous initial guess (IG) trajectory. An optimization problem is then formulated for determining control histories, which enforce continuity of the transfer, while minimizing some scalar objective function J. This problem is solved directly by dividing the IG into $2M$ controlled segments (M segments for the unstable manifold portion, and similarly for the stable portion), while reserving some initial duration (along each branch) to remain uncontrolled. Next, $\phi_i(t)$ or $q_i(t)$ and $\mathbf{u}_i(t)$ are approximated (for each i craft in formation), piecewise over each segment, using a finite number of parameters. These approximations may include some combination of the following terms: constant, polynomial of some order and piecewise regularity, trigonometric in time or some other variable. For these assumptions and objectives, the following generalized procedure is proposed to formulate and solve optimal Coulomb reconfigurations:

1. Globalize the starting configuration unstable manifold ($\mathbf{X^u} \subset W^u$) and target configuration stable manifold ($\mathbf{X^s} \subset W^s$). Then let $\mathbf{X^u}_{ij}$ and $\mathbf{X^s}_{ij}$ denote manifold state vectors for a particular node β_j and propagation times t^u_i and t^s_i. Where, the time bounds $t^{u/s}_{min}$ and $t^{u/s}_{max}$, given by Eq. (8), are to be specified as inputs.

$$t^u_{min} \leq t^u_i \leq t^u_{max} \qquad t^s_{min} \leq t^s_i \leq t^s_{max} \tag{8}$$

2. Define $\vec{\Psi} = \mathbf{X^s}_{ij} - \mathbf{X^u}_{ij}$ as the manifold state discontinuity vector for each: t^u_i, t^s_i, and β_j. Find times $t^u_{tot} \in \{t^u_{min}, t^u_1, \dots, t^u_{max}\}$ and $t^s_{tot} \in \{t^s_{min}, t^s_1, \dots, t^s_{max}\}$ (and β_j values where

applicable) such that a scalar weighted norm function of $\vec{\Psi}$ (denoted ψ) is minimized. These times then define a patch point t_f, at which $\vec{\Psi}$ must be driven to zero for a continuous transfer. This provides the discontinuous IG, which is on the unstable manifold for $t : 0 \rightarrow (t^u_{tot} = t_f)$, and on the stable manifold for $t : t_f \rightarrow (t^s_{tot} + t_f)$.

3. The number of control segments M and segment start times (τ^u_j and τ^s_j, subject to Eqs. (9a)-(9a)) are also specified by the user, and the uncontrolled duration of the transfer is generally selected to be large (i.e. $t_f - \tau^u_1 \ll t^u_{tot}$ and $\tau^s_1 - t_f \ll t^s_{tot}$).

$$t_0 < \tau^u_j < \tau^u_{j+1} < t_f \qquad t_f < \tau^s_{j+1} < \tau^s_j < (t_f + t^s_{tot}) \tag{9a}$$

$$\forall\, j \in \{1 \ldots M-1\} \tag{9b}$$

4. A vector of independent decision variables $\mathbf{X_p}$ is selected, along with upper/lower bounds for each element, with the variables (or parameters) consisting of combinations of the following:

   - Impulsive changes to each s/c $\mathbf{X}$ (e.g. $\Delta\mathbf{v}$)
   - Some parameterization for approximating the s/c control functions (i.e. charge control and inertial thrust), over each segment.
   - Segment start times (τ^u_j and τ^s_j) and total manifold propagation times (t^u_{tot} and t^s_{tot}).

5. A nonlinear programming method is then used to iterate on $\mathbf{X_p}$ in order to minimize some J, subject to $\vec{\Psi} = 0$ (and any other problem specific constraints).

Possible Permutations of the Optimal Transfer Problems

Transfers involving an assortment of Coulomb formations (e.g. number of s/c, s/c masses, force model, $\mathbf{X}^*$ as equilibrium or periodic, ect), with various optimization formulations, are within the scope of the general procedure. Some particularly interesting permutations to the problem formulation, for validating and testing the proposed methodology include:

1. Time(s) free or fixed (τ_j, $t^{u/s}_{tot}$ variables in $\mathbf{X_p}$), value of M, and the $t^{u/s}_{min}$ and $t^{u/s}_{max}$ limits.
2. What elements of $\mathbf{X}$ require continuity (defines $\vec{\Psi}$), and how ψ is computed.
3. The number of manifolds branches: generated, optimized simultaneously, and controlled.
4. What performance index J is used: power, total ΔV, or fuel use.
5. How inertial and Coulomb thrusting systems are modeled (chemical, EP, VSI/CSI), parameterized, and the bounds placed on the parameters.
6. Path constraints on $\mathbf{u}(t)$ and/or $\mathbf{X}(t)$ (of particular interest is to ensure $\mathbf{u}(t)$ is nearly orthogonal to all s/c relative position vectors to prevent thruster plume impingement).

PARTICLE SWARM OPTIMIZATION

The generalized methodology of the previous section formulated the optimal Coulomb reconfigurations as nonlinear programming problems, whose methods of solution can be classified as either deterministic or stochastic. Deterministic or gradient methods generally require derivatives of J with respect to $\mathbf{X_p}$, and an initial guess (IG) for $\mathbf{X_p}$ that is within some unknown convergence tolerance, whereas stochastic methods generally require neither. A gradient method was initially attempted in this research; however, several numerical difficulties arose, resulting in an inability to converge, even for relatively simple Coulomb formation transfers. Furthermore, it is highly non-intuitive to provide quality guesses for s/c potential histories $\phi_i(t)$ and segment start times τ_j, necessitated by such methods. The numerical issues are likely the result of: vastly different orders of magnitude (and response time) between state variables $\mathbf{X}$ and variables associated with electric potentials, high-sensitivity of the manifolds, and error accumulated during propagation of analytical gradients. With significant effort devoted to proper tuning and scaling, the numerical obstacles might be resolved; however, this method type was abandoned in favor of a stochastic method, thereby avoiding those numerical and quality IG generation difficulties.

The stochastic method adopted for this research, is a variation of Particle Swarm Optimization (PSO), first introduced by Kennedy and Eberhart[12] and inspired by the motion of bird flocks searching for food. Pontani and Conway (among others) have successfully applied PSO to optimal spacecraft trajectory problems including: impulsive and finite-burn transfers, low-thrust maneuvers, and targeting of Lyapunov orbit conditions in the CRTBP.[13] In addition to providing persuasive evidence of the method's adeptness for solving the generalized optimal reconfigurations, these works indicate PSO to be equally useful in the numerical determination of yet unknown Coulomb formation equilibrium/periodicity conditions.[13]

Moreover, PSO is often able to avoid local minima (unlike gradient methods) and in contrast to other stochastic methods it is very simple to implement. Its minor drawbacks include occasional difficulty in handling/satisfying constraints and an increase in computational complexity (relative to gradient methods).[13] Specified bounds on the elements of $\mathbf{X_p}$ are required by PSO, but this requirement is well suited for Coulomb transfers, since the controls are physically limited by s/c hardware (e.g. power supply and thruster gimbals). Therefore reasonable bounds may be justified using simple analytical expressions, and such selections are discussed when pertinent. The PSO implementation utilized in this work, closely follows that of,[13] and is summarized as follows:

1. **Generate Initial Random Population**

   A population of M_{pop} individuals is created, each with a corresponding parameter vector $\mathbf{X_p}$ and an update/direction vector $\delta\mathbf{X_p}$. The $\mathbf{X_p}$ components are uniformly and randomly generated within specified upper and lower bounds, and the $\delta\mathbf{X_p}$ components are generated similarly with bounds equal to the $\pm$ of the corresponding $\mathbf{X_p}$ component range.

2. **Begin Iteration, at** $l_0 = 1$

3. **Augmented Performance Index** $\tilde{J}$ **is computed for each individual at iterate** l

   The performance index J is augmented with penalty function terms to account for and handle constraints. Equality constraints ($D_k = 0$, for $k = 1 \ldots K$) are treated according to Eq. (10a), where the weights α_k must be provided as inputs to the algorithm. Inequality constraints are

handled differently as specified by Eq. (10b), where a very large $\tilde{J}$ is assigned if any inequality is violated, thereby enforcing feasibility.

$$\tilde{J} = J + \sum_{k=1}^{K} \alpha_k \left| D_k(\mathbf{X_p}) \right| \tag{10a}$$

$$\text{Inequality Violation :} \qquad \tilde{J} = \infty \qquad \delta\mathbf{X_p}(l) = 0 \tag{10b}$$

4. **Update $\mathbf{X_p}$ from $\delta\mathbf{X_p}$ and Enforce Bounds**

   The best parameter vector (yielding lowest $\tilde{J}$) for each i individual (from $l_0 \dots l$) is denoted $\mathbf{Z_p^i}$. And the best parameter vector for the entire population (from $l_0 \dots l$) is denoted $\mathbf{Z_{min}}$ (with global best cost $\tilde{J}_{min}$). Each individuals direction and parameter vectors ($\delta\mathbf{X_p}(l+1)$ and $\mathbf{X_p}(l+1)$) are then updated according to Eqs. (11a)-(11c).

$$\delta\mathbf{X_p}(l+1) = C_I \delta\mathbf{X_p}(l) \; + C_C \left[\mathbf{Z_p}(l) - \mathbf{X_p}(l)\right] \; C_S \left[\mathbf{Z_{min}}(l) - \mathbf{X_p}(l)\right] \tag{11a}$$

$$C_C = 1.49445 r_2(0,1) \qquad C_S = 1.49445 r_3(0,1) \qquad C_I = \frac{1 + r_1(0,1)}{2} \tag{11b}$$

$$\mathbf{X_p}(l+1) = \mathbf{X_p}(l) + \delta\mathbf{X_p}(l+1) \tag{11c}$$

   Where the terms: r_1, r_2, and r_3 are independent uniform random-numbers distributed over the interval $(0,1)$, and computed at each l, and the terms: C_I, C_C, C_S are inertial, cognitive, and social heuristics, respectively. Therefore, C_I tends to maintain the current direction $\delta\mathbf{X_p}(l)$, C_C tends to move the individual towards its personal best, and C_S tends to move the individual towards the population best. After the update, each component of $\delta\mathbf{X_p}(l+1)$ is forced to be within its bounds. Furthermore, if any $\mathbf{X_p}$ component violates its bound, that element is set to be on-boundary, and its corresponding $\delta\mathbf{X_p}$ component is set equal to zero.

Pontani and Conway use the heuristic functions of Eq. (11b) (these have been optimized, for various problems, during early PSO performance research), and their procedure stops when a max number of iterations is reached.[13] In this work, the Eq. (11b) heuristics are also adopted, but an alternate stopping criteria is proposed, where convergence is said to occur when: $\mathbf{Z_{min}}$ satisfies all constraints to some tolerance (ϵ_1), and the average $\tilde{J}$ of the entire population is within a small tolerance (ϵ_2) of $\tilde{J}_{min}$. The few variables that must be tuned when using this method are: α_k, M_{pop}, and parameter bounds. The most problematic tuning when applied to Coulomb formation transfers along manifolds is the selection of the α_k values (penalty function weights). The PSO method has difficulty converging to a continuous transfer (i.e. in satisfying $\vec{\Psi} = 0$) when the order of magnitude of any of these weights are set improperly.

NUMERICAL TEST CASES: OPTIMAL COULOMB FORMATION RECONFIGURATIONS

In this section, the generalized methodology for formulating and optimizing Coulomb formation reconfigurations is numerically demonstrated using test cases associated with the 2-s/c Radial and Orbit-Normal equilibria (the Along-Track is emitted due to the lack of unstable/stable modes in the linearized system). The values in Table 2 are used for all numerical results, and closely follow those used by Natarajan and Schaub in their work on targeting such transfers.[9] Additionally, only s/c 1 trajectories are considered in optimizing the transfers, since the CM condition of the Hill

Table 2. Input Parameters used in Manifold Generation and Numerical Simulations

Parameter	Value	Units
R_{sc}	1	meters
λ_d	180	meters
a_0	4.227×10^7	meters
ω	7.2593×10^{-5}	rad/sec
k_c	8.99×10^9	$\frac{Nm^2}{C^2}$
$m_1 = m_2$	150	kg

frame model explicitly ensures the continuous transfer of s/c 2. Once optimal reconfigurations are converged, these trajectories are propagated forward in time to ensure that complete transfers are, in fact, achieved.

Invariant Manifold Examples for the Radial and Orbit-Normal Configurations

Following the aforementioned procedure, global invariant manifolds associated with the 2-s/c Radial and Orbit-Normal configurations are generated, using $L_0 = 25$ m and integer values of the reference (CM) orbital period T_p for the propagation times. All manifolds branches are initiated using a perturbation magnitude of $\epsilon = 1.0e^{-5}$ (perturbations to velocity only so as to simulate an initial $\Delta\mathbf{v}$), and it should be noted that an increased ϵ value would result in further evolution of the manifold for the same propagation time. Although the manifolds do depend on parameters (i.e. ω, m_1, and m_2), those illustrated in Figures 4(a)-5(b) do represent the general manifold structures (independent of ω, m_1, and m_2), since no bifurcations occur in the eigenspaces of these systems.

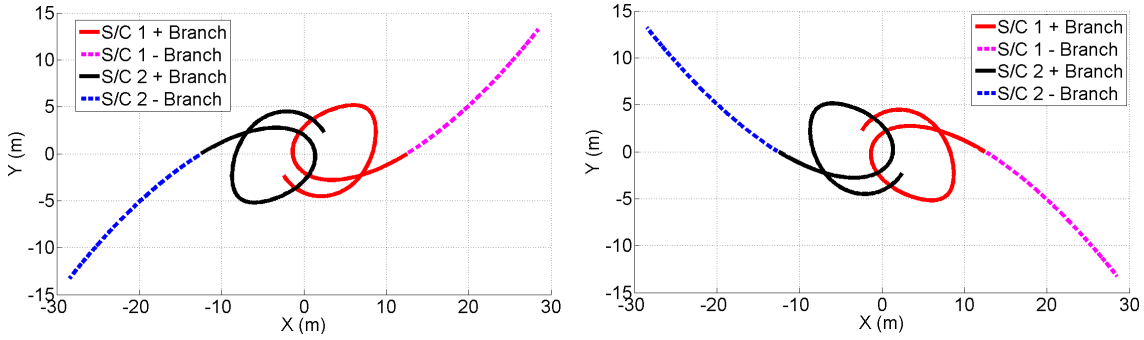

(a) Stable Manifolds (b) Unstable Manifolds

Figure 4. Radial Configuration Manifolds in Rotating Frame: Propagated with CW EOM for 1 T_p

There is substantial symmetry in each s/c manifold branch as well as between stable and unstable manifolds. The Orbit-Normal configuration manifolds are seen to exhibit an oscillatory frequency in the x-y plane, and another along the z-axis (resulting in multiple crossings or piercings of the x-y plane). Next, it is noted that the invariant manifolds associated with the Radial configuration are planar and Figures 4(a)-4(b) suggest that nearly tangential crossings of stable with unstable manifold branches are likely (particularly for the half-manifold which spiral inward). Because of these observations, it is sensible to begin with transfers from one Radial configuration to another,

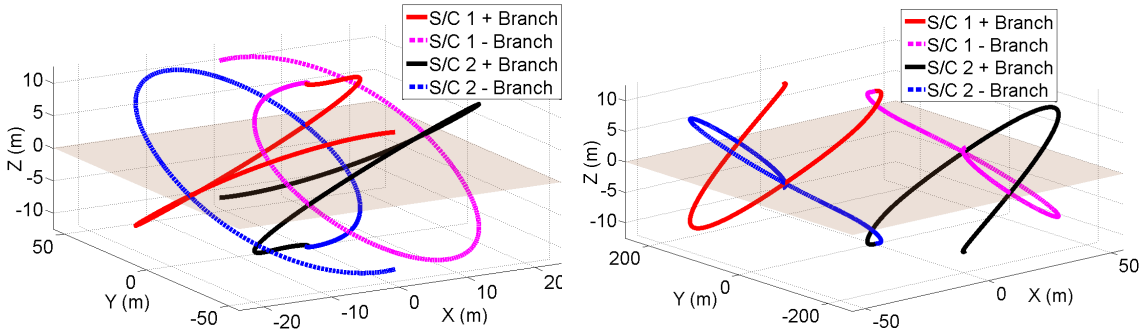

(a) Stable Manifolds (b) Unstable Manifolds

Figure 5. Orbit-Normal Manifolds in Rotating Frame: Propagated with CW EOM for 3 T_p

which can be expansions (increase in L) or contractions (decrease in L).

Finally, in order to validate the accuracy of the CW linearized gravitational model, the classical Newtonian gravitational acceleration is used (along with the Coulomb acceleration) in the numerical integration of the dynamical system. The resulting s/c state histories transformed from inertial to Hill frame, yield manifolds (not shown) nearly identical to those of Figures 4(a)-5(b).

Assumptions and Optimization Model for the Reconfiguration Test Cases

A limited subset of the many permutations discussed in the generalized optimization methodology are tested here. The major assumptions/restrictions used in generating the numerical results provided may be summarized as follows:

1. Only time-fixed optimal transfers are considered, with equally spaced control segments, and manifold propagation bounds of: $t^u_{max} = t^s_{max} = 2\,T_p$ and $t^u_{min} = t^s_{min} = T_p$ (which bounds the total transfer time to be between: $2 - 4\,T_p$ or approximately $2 - 4$ days).
2. The only constraints on the problem is to match continuity at the patch point (i.e. $\vec{\Psi} = 0$).
3. The charge control is modeled using a constant perturbation δq_j from the nominal q_{ref}, over the segment j, that is: $q_j(t) = q_{ref}\,(1 + \delta q_j)$, for $j = 1 \ldots M$
4. Inertial thrusting is modeled with impulsive $\Delta\mathbf{v}_j$ maneuvers occurring at the $M + 1$ control segment nodes, and the performance index J is: $J = \sum_{j=1}^{M+1} \|\Delta\mathbf{v}_j\|$

Assuming instantaneous q (or ϕ) changes is reasonable so long as $|\delta q_j|$ is bounded such that steady-state is reached on a time-scale much less than the s/c dynamical response, for the minimum allowable emission current $|I_{out}| \geq |I_{en}|$. This bound is given by Eq. (12a), where a maximum charge transition time of $(\Delta t_q)_{max} \leq 1$ ms is assumed, and $|I_{en}| = 10\mu A$ is inferred from experimental data.[2] Another upper bound, as given by Eq. (12b), may be established via Eq. (3), by enforcing a maximum power requirement P_{max}.

$$|\delta q_j|_{max} = \frac{(\Delta t_q)_{max}\; I_{out}}{q_{ref}} \tag{12a}$$

$$P_{max} = I_{out}\;\phi_{ref}\,(1 + |\delta\phi|_{max}) = \left(\frac{k_c\; I_{out}}{R_{sc}}\right)\; q_{ref}\,(1 + |\delta q|_{max}) \tag{12b}$$

Also, it must be ensured that these upper limits exceed a lower bound requirement that the impulse is substantial enough to go from the stable equilibrium charge to the unstable equilibrium charge at the patch point (i.e. $|\Delta q_j| = |q_{ref}^{u/s}||\delta q_j| \geq |q_{ref}^{u} - q_{ref}^{s}|$). As an example of using these expressions, consider a Radial configuration with $L_0 = 25$ m and $R_{sc} = 1$ m. Eq. (12a) with $I_{out} = I_{en}$ then yields: $|\delta q_j| \leq 0.0065$, and Eq. (12b) with $P_{max} = 0.15$ W yields: $|\delta q_j| \leq 0.083$. Therefore in this example, the Eq. (12a) bound is more restrictive and therefore is used. Finally, Eq. (13) will define ψ, a weighted norm function of $\vec{\Psi}$, which is minimized in order to determine the manifold propagation times (t_{tot}^{u} and t_{tot}^{s}).

$$\min \psi(t_i^u, t_i^s) = \sqrt{\left[\mathbf{r}^s(t_i^s) - \mathbf{r}^u(t_i^u)\right]^2 + 1000\left[\mathbf{v}^s(t_i^s) - \mathbf{v}^u(t_i^u)\right]^2} \qquad T_p \leq t_i^{u/s} \leq 2\,T_p \qquad (13)$$

Where, t_i^u and t_i^s are unstable and stable manifold propagation times, and $\mathbf{r}^u$/$\mathbf{r}^s$ and $\mathbf{v}^u$/$\mathbf{v}^s$ denote unstable/stable position and velocity vectors at these times.

Optimal Radial Expansion and Contraction Examples

As was noted in Figures 4(a)-4(b), the 2-D nature of the Radial configuration manifolds and likeliness of near cost-free unstable to stable crossings, makes these the simplest transfers to test. Therefore, a Radial expansion ($L_0 = 25$ m and $L_f = 50$ m) and a contraction ($L_0 = 40$ m and $L_f = 15$ m) are demonstrated here. The manifolds for all four configurations are globalized using the limits in Eq. (13) and the minimal ψ is computed numerically for each transfer. This yields the uncontrolled trajectories shown in Figures 6(a)-6(b), which have total transfer times ($t_{tot}^{u} + t_{tot}^{s}$) of approximately: 2.24 days and 2.62 days, respectively.

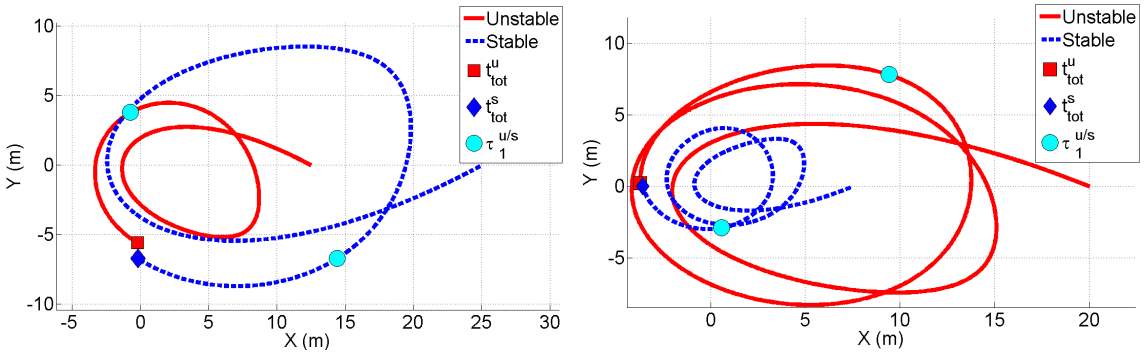

(a) Expansion of: $L = 25 \rightarrow 50$ m

(b) Contraction of: $L = 40 \rightarrow 15$ m

Figure 6. Initial Guess Transfers Between Radial Configurations Along Manifolds

The generalized procedure (with PSO) is then applied to these trajectories, using the assumed optimization problem model with impulsive charge changes, and the parameters defined in Table 3. Also, $t_1^{u/s}$ is selected such that 96% of the total trajectory durations are uncontrolled, and $|\delta q_j| < 0.1$ is chosen (yielding a possible $P_{max} = 20$ W, however the maximum power necessary in the converged solutions is less).

Figures 7(a)-7(b) illustrate the optimal converged expansions, resulting from the application of the method using all parameter values and assumptions previously stated (but Figure 7(a) is the result of a formulation in which only the unstable branch segments are controlled and Figure 7(b)

Table 3. Parameters used for Optimal Radial Expansion and Contraction Results

Control Segs., M	Pop. Size M_{pop}	Tolerance on $\vec{\Psi}$, ϵ_1	PSO stop tol., ϵ_2	Max. Interior $\lvert\Delta v\rvert$ (mm/s)	Max. Final $\lvert\Delta v\rvert$ (cm/s)	Pos./Vel. Penalty Weights, α_k
3	20	$1.0e^{-10}$	$1.0e^{-7}$	0.5	1	$1.0e^{3}$ / $1.0e^{5}$

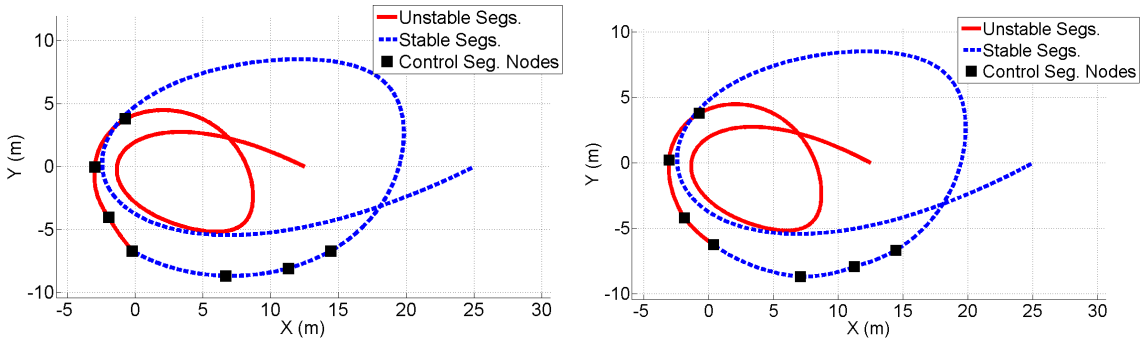

(a) Expansion with Unstable Segs. Control Only (b) Expansion with Both Branches Controlled

Figure 7. Optimal Radial Expansion Transfers ($L = 25 \rightarrow 50$ m)

results from both branches having controlled segments). The formulation using only unstable segment control yielded a lower total impulsive cost ($\Delta V = 6$ mm/sec compared to $\Delta V = 19.45$ mm/sec). Finally, Figure 8 illustrates an optimal contraction, with both branches controlled, and resulted in $\Delta V = 19.44$ mm/sec.

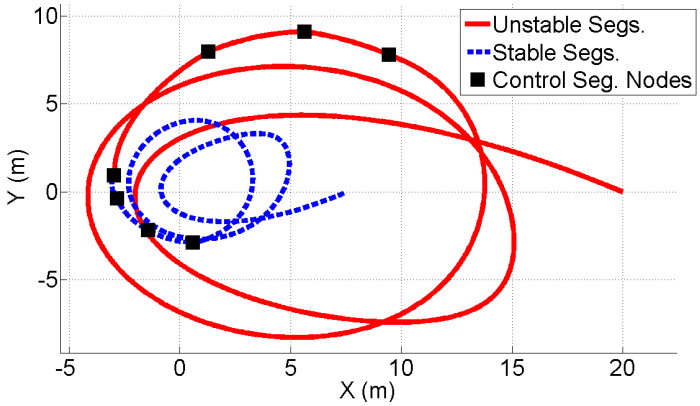

Figure 8. Optimal Radial Contraction Transfer with Both Branches Controlled ($L = 40 \rightarrow 15$ m)

Orbit-Normal Configuration Initial Guess Transfers

The manifolds associated with the Orbit-Normal configuration evolve more slowly, due to those modes having oscillatory parts, and therefore reconfigurations involving them will generally require more time. Figure 9(a) shows an IG trajectory for an Orbit-Normal expansion from $L_0 = 25$ m to $L_f = 50$ m, resulting from the minimization of ψ (as defined in Eq. (13)), and yields a total transfer duration of approximately 4 days. Also, Figures 5(a)-5(b) show that the Orbit-Normal manifolds have multiple piercings of the $x - y$ plane, with bounded z components. This suggests

that the Radial and Orbit-Normal manifolds may reasonably contribute to transferring between these configurations, and therefore lend themselves to the generalized optimization method. An example of this is shown in Figure 9(b), for a starting Radial configuration with $L_0 = 10$ m and a target Orbit-Normal configuration with $L_f = 50$ m (total duration of approximately 5.23 days).

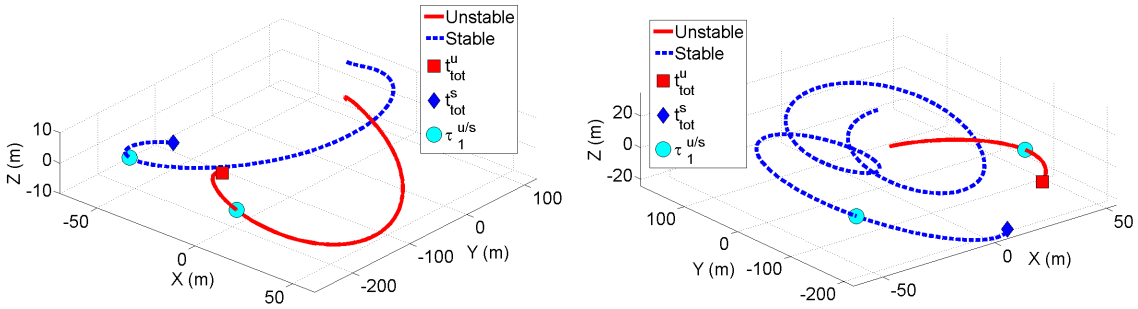

(a) Orbit-Normal Expansion $L = 25 \rightarrow 50$ m

(b) Radial to Orbit-Normal Expansion $L = 10 \rightarrow 50$ m

Figure 9. Initial Guess Transfers involving Orbit-Normal Configuration Manifolds

These IG transfers are presented in order to illustrate one direction this research is headed in, and to indicate some of the difficulties and challenges that are being addressed.

CONCLUSIONS AND FUTURE STUDIES

Active charge control of closely-flying spacecraft (s/c), result in Coulomb forces which supply a nearly propellant-less propulsion system, that avoids the problem of thruster impingement. These charged s/c swarms admit numerous equilibrium configurations, that render 'virtual structures', often referred to as Coulomb formations. In the current work, a generalized method has been developed for formulating and solving optimal transfers from one Coulomb configuration to another. The method exploits uncontrolled flow along invariant manifolds to complete as much of the trajectory as possible, and therefore is only really useful in minimizing consumables as opposed to time, since manifold flows are long duration in nature. A unique stochastic method (referred to as PSO), inspired by the randomized motion of bird flocks, is used to solve the optimal reconfiguration problems. Numerical results are presented as demonstrative examples of the general reconfiguration procedure (and stochastic method) using a simple 2-s/c Coulomb formation model.

This research has provided the general method groundwork, but it is currently unclear how tuning of the stochastic method and optimization problem formulation might effect the quality of the solution; and therefore, more permutations must be explored to answer this question. Also, extended testing of the method would further validate its generality, including transfers for which: different configurations (including those with more than 2-s/c) are involved, inertial thrusting is constrained to be normal (or nearly) to the s/c line-of-sight vectors, continuous control functions are used. Additional applications for Coulomb formation invariant manifolds are discussed, including their centrality in the derivation of a class of discrete station-keeping methods. Advantages of using the PSO method, as opposed to gradient based methods, in solving the reconfiguration problems, are outlined. Finally, future work will apply PSO to the numerical determination of yet undiscovered Coulomb formation equilibrium and periodicity conditions (for constant and/or variable charge), a task for which the method seems well-suited.

REFERENCES

[1] Lawson, P.R. and Dooley, J.A., "Technology Plan for the Terrestrial Planet Finder Interferometer," Tech. Rep. JPL Publication 05-5, NASA Jet Propulsion Lab, June 2005.

[2] King, L.B., Parker, C.G., Deshmukh S. and Chong J., "Spacecraft Formation-flying using Inter-vehicle Coulomb Forces," NIAC - NASA Institute for Advanced Concepts Technical Report, January 7th 2002.

[3] King, L.B., Parker, C.G., Deshmukh S. and Chong J., "Study of Interspacecraft Coulomb Forces and Implications for Formation Flying," *Journal of Propulsion and Power*, Vol. 19, No. 3, 2003, pp. 497-505.

[4] Berryman, J., and Schaub, H., "Analytical Charge Analysis for Two- and Three-Craft Coulomb Formations," *Journal of Guidance, Control, and Dynamics*, Vol. 30, No. 6, Nov-Dec 2007.

[5] Mullen, E. G., Gussenhoven, M. S., and Hardy, D. A.,"SCATHA Survey of High-Voltage Spacecraft Charging in Sunlight," *Journal of the Geophysical Sciences*, Vol. 91, No. A2, 1986, pp. 14741490.

[6] Whipple, E. C., and Olsen, R. C., "Importance of Differential Charging for Controlling Both Natural and Induced Vehicle Potentials on ATS-5 and ATS-6," *Proceedings of the 3rd Spacecraft Charging Technology Conference*, NASA CP 2182, 1980, p. 887.

[7] Escoubet, C.P., Fehringer, M., and Goldstein, M., "The Cluster Mission," *Annales Geophysicae*, Vol. 19, No. 10/12, 2001, pp. 11971200.

[8] Schaub, H., Kim, M., "Orbit Element Difference Constraints for Coulomb Satellite Formations," *AAS/AIAA Astrodynamics Specialist Conference*, AIAA Paper 04-5213, 2004.

[9] Natajaran, A., and Schaub, H., "Hybrid Control of Orbit Normal and Along-Track 2-Craft Coulomb Tethers," *AAS/AIAA Space Flight Mechanics Meeting*, AAS 07-193, Sedona, Arizona, Jan.-Feb. 2007.

[10] Inampudi, R., "Two-Craft Coulomb Formation Study About Circular Orbits and Libration Points," PhD Dissertation, 2010.

[11] Hogan, E. and Schaub, H., "Collinear Invariant Shapes for Three-Craft Coulomb Formations," *AAS/AIAA Astrodynamics Specialists Conference*, AIAA 2010-7954, Toronto, Ontario, August 2010.

[12] Kennedy, J., and Eberhart, R., "Particle Swarm Optimization," *Proceedings of the IEEE International Conference on Neural Networks*, Piscataway, NJ, 1995, pp. 19421948.

[13] Pontani, M., and Conway, B.A., "Particle Swarm Optimization Applied to Space Trajectories," *AIAA Journal of Guidance, Control and Dynamics*, Vol. 33, No. 5, Sept.-Oct. 2010, pp. 1429-1441.

[14] Clohessy, W.H. and Wiltshire, R.S., "Terminal Guidance System for Satellite Rendevous," *Journal of the Aerospace Sciences*, Vol. 27, No. 9, 1960, pp. 653-658.

[15] Natarajan, A. and Schaub, H., "Linear Dynamics and Stability Analysis of a Two-Craft Coulomb Tether Formation," *Journal of Guidance, Control, and Dynamics*, Vol. 29, No. 4, July-August 2006, pp. 831-838.

[16] Marchand, B.G., "Spacecraft Formation Keeping Near the Libration Points of the Sun-Earth/Moon System," PhD Dissertation, August, 2004.

[17] Stiles, L., Seubert, C., and Schaub, H., "Effective Coulomb Force Modeling in a Space Environment," *AAS/AIAA Spaceflight Mechanics Meeting*, AAS 2012-105, Charleston, SC, Jan.-Feb. 2012.

[18] Natarajan, A., "A Study of Dynamics and Stability of Two-Craft Coulomb Tether Formations," PhD Dissertation, 2007.

[19] Russell, R.P., and Lam, T., "Designing Ephemeris Capture Trajectories at Europa Using Unstable Periodic Orbits," *Journal of Guidance, Control, and Dynamics*, Vol. 30, No. 2, MarchApril 2007, pp. 482-491.